


Genetic or Toxicant-Induced Disruption of Vesicular Monoamine Storage and Global Metabolic Profiling in *Caenorhabditis elegans*

Joshua M. Bradner,* Vrinda Kalia,* Fion K. Lau,* Monica Sharma,*
Meghan L. Bucher,* Michelle Johnson,[†] Merry Chen,[†] Douglas I. Walker,[‡]
Dean P. Jones,[§] and Gary W. Miller ^{*,1}

*Department of Environmental Health Sciences, Mailman School of Public Health, Columbia University, New York, New York 10032, USA; [†]Department of Environmental Health, Rollins School of Public Health, Emory University, Atlanta, Georgia 30322, USA; [‡]Department of Environmental Medicine and Public Health, Icahn School of Medicine at Mount Sinai, New York, New York 10029, USA and [§]Department of Medicine, School of Medicine, Emory University, Atlanta, Georgia 30303, USA

Joshua M. Bradner and Vrinda Kalia contributed equally to this study.

¹To whom correspondence should be addressed at Department of Environmental Health Sciences, Mailman School of Public Health, Columbia University, New York, NY 10032. E-mail: gary.miller@columbia.edu.

ABSTRACT

The proper storage and release of monoamines contributes to a wide range of neuronal activity. Here, we examine the effects of altered vesicular monoamine transport in the nematode *Caenorhabditis elegans*. The gene *cat-1* is responsible for the encoding of the vesicular monoamine transporter (VMAT) in *C. elegans* and is analogous to the mammalian vesicular monoamine transporter 2 (VMAT2). Our laboratory has previously shown that reduced VMAT2 activity confers vulnerability on catecholamine neurons in mice. The purpose of this article was to determine whether this function is conserved and to determine the impact of reduced VMAT activity in *C. elegans*. Here we show that deletion of *cat-1*/VMAT increases sensitivity to the neurotoxicant 1-methyl-4-phenylpyridinium (MPP⁺) as measured by enhanced degeneration of dopamine neurons. Reduced *cat-1*/VMAT also induces changes in dopamine-mediated behaviors. High-resolution mass spectrometry-based metabolomics in the whole organism reveals changes in amino acid metabolism, including tyrosine metabolism in the *cat-1*/VMAT mutants. Treatment with MPP⁺ disrupted tryptophan metabolism. Both conditions altered glycerophospholipid metabolism, suggesting a convergent pathway of neuronal dysfunction. Our results demonstrate the evolutionarily conserved nature of monoamine function in *C. elegans* and further suggest that high-resolution mass spectrometry-based metabolomics can be used in this model to study environmental and genetic contributors to complex human disease.

Key words: VMAT; vesicle; monoamine; MPP⁺; neurodegeneration; *cat-1*; metabolomics; high-resolution mass spectrometry.

The synaptic vesicle plays a significant role in the protection of neurons from toxic insult. The vesicular amine transporters (VATs) are members of the toxin extruding antiporter (TEXAN) gene family of proton antiporters, closely related to proteins in prokaryotic organisms that work to exclude antibiotics from the cytoplasm (Parsons, 2000; Schuldiner et al., 1995). In eukaryotes, members of this family reside on the inner vesicular membrane and are instrumental in packaging neurotransmitters into synaptic vesicles, ensuring the transmission of the action potential. Additionally, these transporters have cytoprotective effects, keeping potentially toxic byproducts of neurotransmitters out of the cytoplasm (vesicular monoamine transporter 2, VMAT2) and ensuring the replenishment of amine stores of acetylcholine in the synaptic cleft (vesicular acetylcholine transporter, VAcHT). The breakdown in this relationship can have potentially deadly results. The adequate release of acetylcholine into the synapse is dependent on the VAcHT. Impairment of acetylcholine release into the synaptic cleft, either through direct inhibition of VAcHT (using vesamicol) or indirectly (using botulinum toxin) can lead to respiratory failure and death (Burton et al., 1994; Dressler et al., 2005; Prior et al., 1992). For other members of the TEXAN family, the breakdown of antiporter activity in synaptic vesicles appears to result in direct toxicity to the cell from oxidized amines, like oxidized metabolites of dopamine (Spina and Cohen, 1989).

When its storage is dysregulated, dopamine can accumulate in the cytosol where it is vulnerable to oxidation and enzymatic catabolism. These processes generate reactive metabolites, such as the dopamine quinone, as well as oxidative stress-inducing reactive oxygen species (Stokes et al., 1999) and catechol aldehydes (Goldstein et al., 2013; Vermeer et al., 2012). Through the utility of mouse, *in vitro* vesicular uptake, and cell culture models, we have established considerable evidence that VMAT2 confers resistance to toxic insult in dopaminergic neurons as a graded response in vesicular function (Caudle et al., 2007; Fumagalli et al., 1999; Lohr et al., 2014, 2015, 2016). We have proposed that increase in VMAT2 leads to a proportional increase in the storage capacity of monoaminergic synaptic vesicles (Lohr et al., 2014). This in turn provides increased protection from both 1-methyl-4-phenyl-1,2,3,6-tetrahydropyridine (MPTP) and *N*-methylamphetamine toxicity (Lohr et al., 2014, 2015, 2016). Others have demonstrated similar results including VMAT2-mediated protection against L-DOPA (the precursor to dopamine) and Parkinson's disease (PD)-associated toxicants (Lawal et al., 2010; Mosharov et al., 2009; Munoz et al., 2012). The hypothesis that increased vesicular sequestration capacity is able to protect against endogenous and exogenous toxicants has been supported in human studies that show a reduction in PD risk associated with gain of function haplotypes in the promoter region of VMAT2 (Brighina et al., 2013; Glatt et al., 2006).

Recent findings highlight VMAT2 as a vulnerable target to environmental toxicants (Caudle, 2015; Caudle et al., 2012). Animal studies suggest that a range of chemical exposures including pesticides, fungicides, polychlorinated biphenyls, polybrominated diphenyl ethers, and perfluorinated compounds reduce the expression and function of VMAT2 and lead to symptoms closely resembling PD (Bradner et al., 2013; Caudle et al., 2005; Choi et al., 2015; Enayah et al., 2018; Inamdar et al., 2013; Miller et al., 1999; Patel et al., 2016; Pham-Lake et al., 2017; Richardson et al., 2006, 2008; Richardson and Miller, 2004; Schuh et al., 2009; Wilson et al., 2014; Xiong et al., 2016). Continued research into the effects of these chemicals on the function of amine transporters should improve our understanding of how

they function to disrupt the vesicular integrity of the synaptic vesicle.

Despite the notable benefits of mouse and *in vitro* cell culture models, changes in behavior and alterations in whole organism metabolic function are difficult and costly to perform in mammalian models. As such, our lab has begun using *C. elegans* as a model to measure neurotoxic outcomes as mediated by a protein 49% identical to VMAT2, a monoamine transporter encoded by the gene *cat-1* (Duerr et al., 1999). In this manuscript, we evaluate the effects of the *cat-1* (*ok411*) mutant allele on *cat-1*/VMAT expression, dopamine neuron integrity, and monoamine-dependent behaviors. We also determined the effects of reduced *cat-1*/VMAT on vulnerability to the classical PD-associated toxicant 1-methyl-4-phenylpyridinium (MPP⁺). Finally, we use high-resolution mass spectrometry-based metabolomics to determine the impact of *cat-1*/VMAT reduction or MPP⁺ treatment on metabolism, measured using the whole organism.

MATERIALS AND METHODS

Reagents

Except where noted, all reagents were purchased from Sigma Aldrich (St Louis, Missouri).

Phylogenetic Relationships of Vesicular Amine Transporters

Sequences of VATs (Supplementary Data 1) from various species were subjected to cladistic organization via bioinformatics online tools located at www.phylogeny.fr (Dereeper et al., 2008).

Strains and Culture Conditions

Long established standard methods of culture including the use of normal growth media (NGM) plates, culture temperatures of 20°C, and the OP50 *E. coli* strain as a food source were followed as described (Brenner, 1974). Deviations in this practice are mentioned in conjunction with the relevant assay. *C. elegans* strains were provided by the CGC, which is funded by NIH Office of Research Infrastructure Programs (P40 OD010440). These include the wild-type N2 Bristol strain, *dat-1* (*ok157*) mutant strain, *daf-16* (CF1038) mutant strain, *cat-2* (CB1112) mutant strain, RB681 [*cat-1(ok411)*] mutant strain, the fluorescent transgenic strain BZ555 (*pDAT::GFP*), and a cross between strain RB681 and BZ555 [*pDAT::GFP*; *cat-1(ok411)*] created in our lab.

All nematodes (hereafter referred to as worms) used in experiments were synchronized at the L1 stage using a bleach/sodium hydroxide mixture optimized following standard techniques (Porta-de-la-Riva et al., 2012). Worms reared in liquid culture were maintained on a shaker set to 120 rpm, at 20°C. Liquid cultures were maintained in S-complete media and fed using the UV-sensitive strain NEC937, following UV exposure per N. Stroustrup (CRG, Barcelona, personal communication).

Genotyping

Strains sourced from the CGC and those resulting from an in-house cross were genotyped using standard polymerase chain reaction (PCR) techniques. Primers used to check the *cat-1* (*ok411*) mutant allele are found in the description listing for strain RB681 on the website for the CGC (Caenorhabditis Genetics Center, 2020).

Western Blot

To visualize the *cat-1*/VMAT protein, *C. elegans* strains N2, *daf-16* (CF1038), *cat-1* (*ok411*), *cat-2* (CB1112), and *dat-1* (*ok157*) were

cultured on NGM plates. A total of 50 worms of each strain were transferred to a 1.5-ml Eppendorf tube containing 150 μ l of M9. After washing 3 times with M9, the worm pellet was suspended in 25 μ l of M9, snap frozen in liquid nitrogen, and stored at -80°C until use. Prior to analysis, samples were thawed on ice, after which 25 μ l of Laemmli 2 \times sample buffer and proteinase inhibitor cocktail were added and the sample mixtures were placed in a sonicating water bath at room temperature for 2 min and immediately placed in heat block at 95°C for 5 min. Samples were run on a NuPage 10% bis tris gel (Thermo Fisher, Waltham, Massachusetts) and transferred to a PVDF membrane. Nonspecific antibody binding was blocked with a 7.5% milk in tris-buffered saline plus tween solution for 1.5 h at room temperature. The primary antibody used was a polyclonal rabbit anti *cat-1*/VMAT serum generated by Dr Richard Nass (IUSM, Indiana) at a dilution of 1:1000. The Secondary antibody used was a goat anti-rabbit HRP-conjugated at a dilution of 1:5000 (Jackson ImmunoResearch, West Grove, Pennsylvania).

Immunohistochemistry

The method was based on a previously published Freeze-Cracking protocol unless otherwise specified (Duerr, 2013). Poly-L-lysine coated slides were prepared to bind worms to slides. Approximately 5000 worms per strain were used to prepare multiple slides. A Fisherbrand Cooling Cartridge (Thermo Fisher, Waltham, Massachusetts) prechilled overnight in -80°C was used to freeze the slides. The slides were lightly fixed using the methanol-acetone method. Nonspecific antibody binding was blocked with a 10% Goat Serum (Thermo Fisher, Waltham, Massachusetts) overnight at 4°C . The primary antibody used was a polyclonal rabbit anti *cat-1*/VMAT serum generated by Dr Richard Nass (IUSM, Indiana) at a dilution of 1:100. The secondary antibody used was Goat anti-Rabbit IgG (H+L) Cross-Adsorbed Secondary Antibody, Alexa Fluor 488 (Thermo Fisher, Waltham, Massachusetts). VECTASHIELD Antifade mounting medium with DAPI (Vector Laboratories, Burlingame, California) was added prior to sealing the coverslips with nail polish. Images were taken at $40\times$ magnification on a Leica DMI8 (Leica, Wetzlar, Germany) inverted epifluorescent microscope.

Analysis of Monoamine-Derived Behaviors

Reserpine is a pharmacological inhibitor of mammalian catecholamine transporters (Deupree and Weaver, 1984). *In vitro* studies looking at [^3H] dopamine uptake in cell culture have shown reserpine to be a potent inhibitor of *C. elegans cat-1*/VMAT as well (Duerr et al., 1999). In this paper, reserpine is used to pharmacologically replicate the loss of *cat-1*/VMAT seen in the *cat-1(ok411)* mutant strain. To create reserpine assay plates, reserpine was dissolved in 1 M acetic acid to a concentration of 50 mM and diluted 1:80 in M9 for a final concentration of 625 μM . Plates without reserpine were exposed to vehicle only (1 M acetic acid diluted 1:80 in M9). A total of 400 μ l was added to the treatment plate and allowed to dry before transferring worms (Duerr et al., 1999). Worms were seeded onto growth plates (6 cm NGM with live OP50) as synchronized L1s and allowed to grow for 48 h. Worms were transferred to reserpine plates and left for 12 h prior to behavioral assays except for egg laying where worms were kept on reserpine plates until the second day of adulthood.

Grazing. Plates for assessing grazing behaviors were created per Duerr et al. (1999). For our assays, worms were rinsed off treatment plates and spotted in 20 μ l of M9 with approximately 100 worms per assay. A lint-free tissue was used to wick away the

M9 and the worms were recorded using a FLIR chameleon 3 camera from Edmund Optics (Barrington, New Jersey) until either the last worm entered the lawn or a maximum of 30 min. Videos were scored by a researcher blind to treatment conditions, measuring the amount of time it took for each worm to enter the lawn of OP50 (tip of nose to end of tail).

Pharyngeal pumping. Pharyngeal contractions were scored by observation of worms through a standard stereomicroscope, using finger taps on an electronic counting application while a timer was running, a method similar to that previously described (Miller et al., 1996).

Wave initiation rate. The celeST software package was used as described to determine aspects of swim behavior for the N2, *cat-1(ok411)* and N2 worms treated with reserpine groups (Restif et al., 2014). Briefly, four worms were placed in 60 μ l of M9 on a glass slide. Recordings of swim behavior were made as a series of jpeg images using a chameleon 3 camera (FLIR; Wilsonville, Oregon) for 30 s at a frame rate of 18 f/s. All subsequent analysis was completely automated using the celeST software package.

Egg laying. For the egg laying assay, retention of eggs inside worms was determined by transferring 2 day adult worms, 1 per well, to 96 well plates containing 20% hypochlorite solution. Dissolution of the worm body and release of eggs was monitored by a researcher blinded to experimental condition and eggs were counted manually.

MPP⁺ Treatment

C. elegans strains, *pDAT::GFP* and *pDAT::GFP; cat-1(ok411)*, were chosen for fluorescent assays due to their intense expression of GFP driven by the *dat-1* promoter, highlighting dopamine neurons. Synchronized worms were grown using standard liquid culture (see above) using 125 ml Erlenmeyer flasks until they reached the YA stage of development. At this point, worms were sorted using confirmed gating parameters into 96 well plates using the COPAS FP-250 large particle flow cytometer (Union Biometrica, Massachusetts) to select for fully developed YA worms. Various concentrations of MPP⁺ dissolved in water were added to the liquid culture (s-complete, UV-treated NEC937, 100 μM Floxuridine), and the worms were left at 20°C on a shaker for an additional 48 h. Worms were then anesthetized in 10 mM sodium azide, mounted on agar (5% in water), and the area surrounding the 6 dopamine neurons in the head were photographed at $20\times$ magnification using a Fisher Scientific EVOS epifluorescence microscope (Waltham, Massachusetts) for later analysis. All photographs were taken using identical objective, light intensity, and exposure settings. We used the Image J software to determine neurodegeneration based on the total area of fluorescence post 48 h of treatment, with the observation that worms treated with MPP⁺ exhibit overall reductions of dopamine neuron size and branching (Schindelin et al., 2012). First, fluorescent photographs were converted into 8-bit grayscale tiff files. Following conversion, the photographs were batch processed using the Yen-automated thresholding algorithm to isolate areas of GFP fluorescence (Yen et al., 1995) creating a binary image of black objects against a white background (Figure 4B). The total area of these objects, representing areas of GFP fluorescence, was calculated using the particle analysis plugin in Image J. Results were combined over 4 experiments as percent area of untreated worms. Statistical testing using two-way ANOVA followed by Bonferroni's multiple comparisons tests were designed to

compare the extent of degeneration between *pDAT::GFP* worms and *pDAT::GFP* worms lacking the *cat-1/VMAT* protein (*pDAT::GFP; cat-1(ok411)*) when treated with equivalent doses of *MPP⁺*. A small series of treatments were run through the COPAS biosorter to get representative fluorescent profiles of worms treated with *MPP⁺*.

High-Resolution Mass Spectrometry-Based Metabolomics. We applied untargeted high-resolution mass spectrometry (HRMS)-based metabolomics to characterize metabolic effects of the *cat-1* mutation and *MPP⁺* exposure in N2 worms. Worms with the *cat-1(ok411)* mutation and wild-type N2 worms were grown in liquid culture as described above and 6 replicates per strain were collected in M9 at the L4 stage and snap frozen in liquid nitrogen. Prior to *MPP⁺* exposure, N2 worms were grown in liquid culture and at the L4 stage, 500 worms were sorted into wells of a 24-well plate using the COPAS FP-250. Worms were exposed to 1 mM *MPP⁺* or the control for 4 h, washed and snap frozen. All samples were stored at -80°C until processed. Metabolites were extracted using acetonitrile (in a 2:1 ratio) which was added to samples along with an internal standard (Soltow et al., 2013). Each sample was placed in the bead beater to disrupt the cuticle, and included shaking at 6.5 m/s for 30 s, cooling on ice for 1 min, and placed in the beater for another 30 s, at the same speed (Mor et al., 2020). All processing was performed on ice or in a cold room when necessary. Untargeted high-resolution mass spectrometry analysis was performed using a dual-chromatography and acetonitrile gradient that included HILIC chromatography with positive electrospray ionization (HILIC-pos) and C18 column with negative electrospray ionization (C18-neg) (Walker et al., 2019). Mass spectral data was generated on a ThermoFischer Q-Exactive HF Orbitrap mass spectrometer operated at 120 000 resolution over mass-to-charge (*m/z*) scan range 85–1250. Data were extracted using the R packages *apLCMS* (Yu et al., 2009) and *xMSanalyzer* (Uppal et al., 2013).

The HILIC positive column measured 21 479 uniquely detected mass spectral features, identified by accurate *m/z*, retention time and intensity in each sample. To focus on detection of endogenous metabolites and pathways related to neurotransmitter metabolism, data analysis was restricted to the HILIC-pos condition only.

***cat-1/VMAT* and *MPP⁺* Metabolome-Wide Association Study.** We analyzed HRMS results using 3 separate approaches to evaluate metabolic alterations due to the *cat-1* mutation and *MPP⁺* exposure: (1) The metabolic effect of the *cat-1* mutation was characterized by comparison to wild-type N2 worms grown under identical conditions. (2) Disruption to worm metabolic function following *MPP⁺* exposure for exposed N2 worms and untreated N2 controls and (3) An overlap analysis was completed by identifying features associated with both *cat-1* and *MPP⁺* for similarities in disruption of systemic metabolic response due to altered dopaminergic neuronal health. A feature was retained in each of the first 2 analyses if its abundance in at least 1 worm sample was 1.5 times its abundance in the M9 buffer used to wash and collect the worms. Prior to data analysis, missing values for each feature were imputed with half the value of the minimum abundance, quantile normalized, \log_{10} transformed, and auto scaled. Features were analyzed using *t* tests, partial least squares discriminant analysis (PLS-DA), hierarchical clustering, and pathway analysis using *mummichog* (Li et al., 2013). All data processing, analysis and visualization was done in R version 3.6.0, using functions: *preprocessCore::normalize.quantiles()* (Bolstad et al., 2003), (*RFmarkerDetector::autoscale()* (Palla, 2015), *gplots::heatmap2()*

(Warnes et al., 2009), *ggplot2::ggplot()* (Wickham, 2016), and *mixOmics::plsda()* (Le Cao, 2016). Pathway analysis was completed using the *Mummichog* algorithm (Li et al., 2013) hosted on the *MetaboAnalyst* (www.metaboanalyst.ca) module “MS peaks to Pathway” (Chong et al., 2019), using the *Caenorhabditis elegans* metabolic reference map available through KEGG. Using output from the *t* tests, a nominal *p*-value cut-off of 0.1 was used to select features for pathway analysis, using a mass tolerance of 5 ppm for *cat-1(ok411)* mutant and for wild-type worms treated with *MPP⁺*. Features that were different between wild-type and *cat-1(ok411)* worms at $p < .1$ (356 features) were compared with features that were different between *MPP⁺* treated and control worms at $p < .1$ (801 features). To discover overlapping features, we used the *getVenn()* function in the *xMSanalyzer* R package with a mass-to-charge tolerance of 5 ppm and retention time tolerance of 5 s. We used the *xMSanalyzer::feat.batch.annotation.KEGG()* function to determine level 4 annotations (Schymanski rating; Schymanski et al., 2014) for the overlapping features (Uppal et al., 2013).

Statistics. All data excluding metabolomics were analyzed using the Graphpad statistical software package (San Diego, California). Behavioral comparisons in Figure 3 were conducted using 1-way ANOVA followed by Tukey’s multiple comparisons tests in cases where $p < .05$. Results from *MPP⁺* assays in Figure 4 were conducted using 2-way ANOVA followed by Bonferroni’s multiple comparisons test. All metabolomic analyses were conducted in R (version 4.0.2).

RESULTS

Phylogenetic Relationships of Vesicular Amine Transporters

Cladistic relationships amongst vertebrate and invertebrate species between the *VMAT(s)* and the *VACHT* are shown in Figure 1.

Genotyping and Protein Analysis of *cat-1(ok411)*

The *ok411* mutant allele was produced by the high throughput *C. elegans* gene knockout consortium (CeDM, 2012). The mutation is a 429 base pair deletion resulting in complete loss of the first coding exon in the *cat-1* gene and a loss of the *cat-1/VMAT* protein by Western blot and immunofluorescence (Figs. 2A–C). A breeding cross of the BZ555 *pDAT::GFP* with the *cat-1(ok411)* mutant was successful in producing a transgenic with the mutant *cat-1(ok411)* allele (Figure 2A). Our efforts at immunostaining support the work of previous labs indicating the expression pattern of *cat-1/VMAT* in the worm (Duerr et al., 1999; Serrano-Saiz et al., 2017).

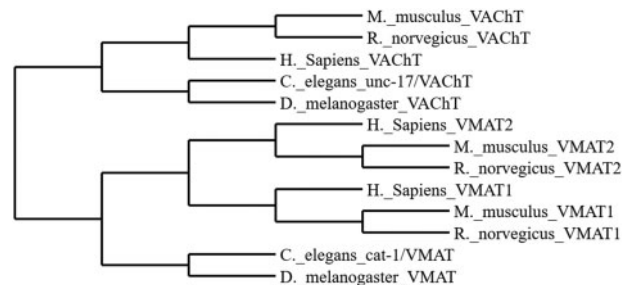


Figure 1. Cladogram representing species specific relationships amongst vesicular amine transporters.

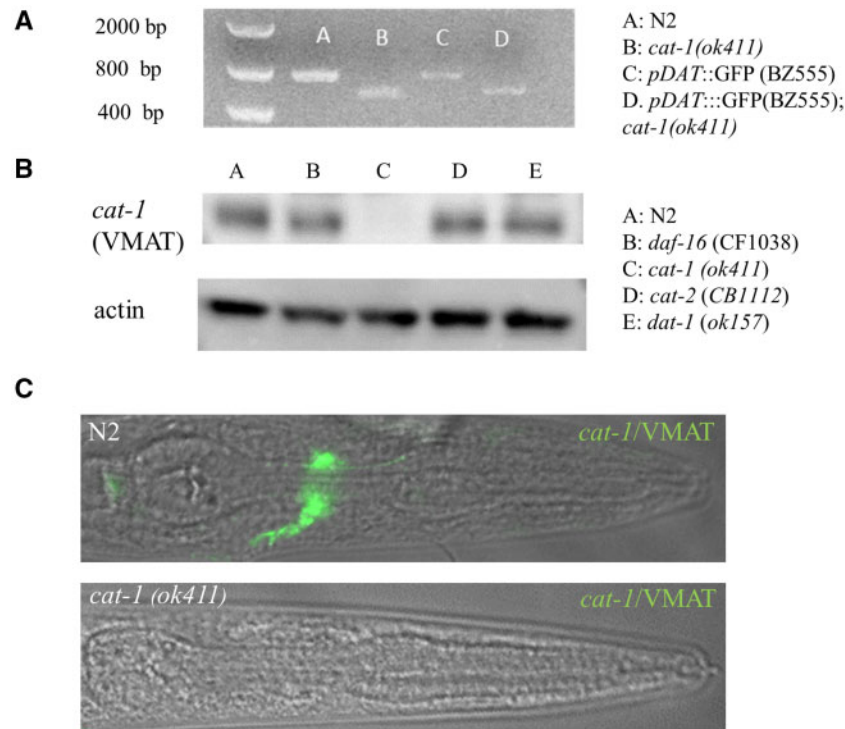


Figure 2. The *cat-1(ok411)* strain is deficient in the production of *cat-1*/VMAT protein. A, Primers specific for *cat-1* reveal a 400bp deletion in the *cat-1(ok411)* mutant strain. B, The strain *cat-1(ok411)* does not produce *cat-1*/VMAT protein. C, The *cat-1(ok411)* strain (B) shows no evidence of *cat-1*/VMAT immunoreactivity (detail of pharyngeal region).

Monoamine-Derived Behaviors

The *cat-1(ok411)* mutant strain lacking *cat-1*/VMAT protein and pharmacological inhibition of *cat-1*/VMAT in N2 worms treated with reserpine demonstrated defective grazing behavior (Figure 3A) indicative of disruption of dopamine and serotonin signaling. In order to determine if this behavior is due to a general difference in motility, we subjected the *cat-1(ok411)* strain and the reserpine treated N2 worms to automated swim behavior analysis using the celeST software and found no significant difference between any of the groups using 10 different measures of stroke analysis including a measure (wave initiation rate measured as: waves/minute) analogous to the thrashing assay (Figure 3D). We employed two measures of serotonergic behaviors; egg laying and pharyngeal pumping. Worms with disrupted serotonergic signaling tend to hold their eggs in *utero* and have a reduced rate of pharyngeal pumping. We found the *cat-1(ok411)* strain and N2 wild type worms treated with reserpine to be both deficient in egg laying behavior and pharyngeal pumping (Figs. 3B and 3C).

MPP⁺ Exposure and Neurodegeneration

Worms treated with MPP⁺ exhibit reductions in total area consistent with the degeneration of dopamine neurons (Figure 4B). Representative fluorescent profiles using the COPAS biosorter support this assertion, MPP⁺ treated worms had shorter intensity peaks for the green channel (Figure 4C). We found that BZ555 transgenic worms lacking *cat-1*/VMAT protein are more susceptible to the toxic effects of MPP⁺ than the BZ555 transgenic worms with *cat-1*/VMAT protein through analysis with 2-way ANOVA, with a significant interaction between strain and dose ($p < .001$) (Figure 4A). Reductions in total GFP area occur at lower concentrations of MPP⁺ in worms with the *cat-1(ok411)* mutant allele.

Metabolomics

There were 114 features (in red) different between the 2 groups with $p < .05$ (Figure 5A). There was also clear clustering of the features with $p < .05$ between the 2 groups (Figure 5B). A metabolome wide association study of phenylalanine metabolism has shown that for initial discovery purposes, raw p combined with metabolic pathway enrichment improves detection of biological effect while reducing identification of false positive biological effects (Go et al., 2015). Thus, for metabolic pathway enrichment, we considered all 356 features with $p < 0.1$. It revealed several metabolic pathways altered with a fisher exact test p -value < 0.1 in the *cat-1(ok411)* mutant (Figure 5C), including tyrosine metabolism (Figure 5C). A partial least squares differential analysis showed separation of the wild-type N2 and *cat-1(ok411)* groups (Figure 5D).

Untargeted metabolomic analysis of worms exposed to MPP⁺ for 4 h was performed similarly to the *cat-1(ok411)* mutant. There were 199 features (in red) significantly different between the treated and untreated groups with $p < .05$ (Figure 6A). These significant features clustered differently in the 2 groups as seen in the heatmap generated using hierarchical clustering analysis (Figure 6B). Pathway analysis using features with $p < .1$ (801 features) was done using mummichog hosted on MetaboAnalyst. It revealed several pathways of interest (Figure 6C), including the tyrosine and tryptophan metabolism pathway, glycerophospholipid metabolism and the pentose glucuronate interconversions pathways (Figure 6C). A partial PLS-DA was able to differentiate between the treatment groups (Figure 6D). Comparing features with $p < .1$ in *cat-1(ok411)* worms and worms exposed to MPP⁺ revealed 14 features altered in both conditions (Supplementary Figure 1). KEGG annotations were made for 2 of the 14 features (Supplementary Table 1) with level 4 confidence according to Schymanski criteria (Schymanski et al., 2014). See supplemental

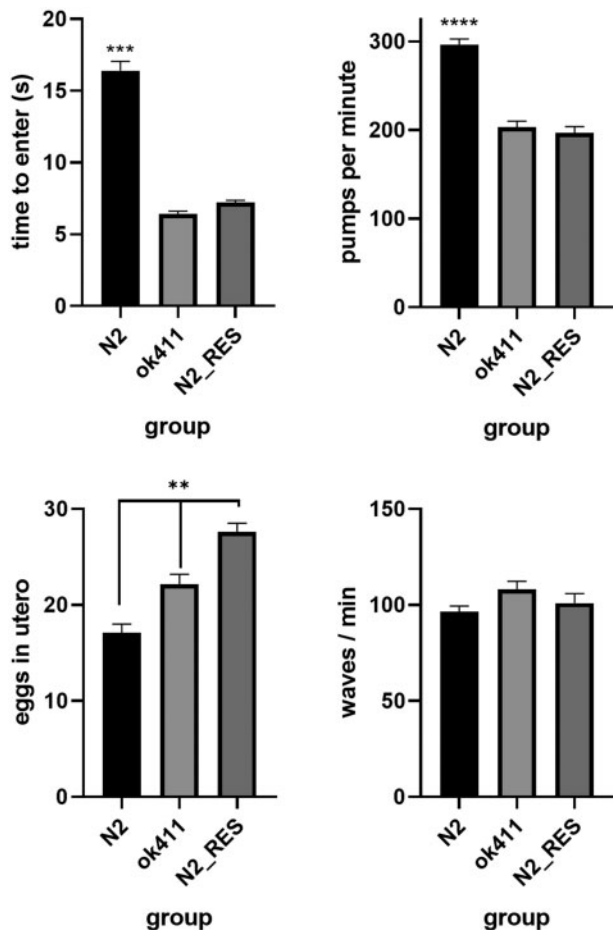


Figure 3. The loss of *cat-1*/VMAT protein results in altered monoaminergic behaviors. A, The grazing response is deficient in the *cat-1* (*ok411*) mutant strain and N2 worms treated with reserpine ($n = 1289$). B, *cat-1* (*ok411*) worms and N2 worms treated with reserpine have impaired pharyngeal pumping compared with N2 ($n = 89$). C, *cat-1* (*ok411*) and N2 worms treated with reserpine are deficient in egg laying (more eggs in utero) ($n = 114$). D, There is no difference in wave initiation between N2 and the *cat-1* (*ok411*) mutant ($n = 55$). N2_res = N2 worms treated with reserpine. All behaviors analyzed using 1-way ANOVA followed by Tukey's multiple comparisons tests where appropriate. ** $p < .01$, *** $p < .001$ vs. all other groups, **** $p < .0001$ vs. all other groups.

excel workbook for raw data at <https://doi.org/10.5061/dryad.0zpc866x0>.

DISCUSSION

The importance of VATs in mitigating catecholaminergic toxicity is well established (Guillot and Miller, 2009; Lohr and Miller, 2014; Spina and Cohen, 1989). Multiple *in vivo* studies have demonstrated the toxic consequences of dopamine including early work that demonstrated toxicity resulting from striatal injections of exogenous dopamine (Hastings et al., 1996). Later studies investigated the consequences of dysregulating endogenous dopamine handling. Overexpression of the plasmalemmal dopamine transporter (DAT) resulted in increased dopamine metabolism and nigrostriatal degeneration thought to result from an accumulation in cytosolic dopamine with insufficient vesicular sequestration capabilities (Masoud et al., 2015). Furthermore, introducing DAT into striatal interneurons that lack the proper machinery to sequester dopamine within vesicles resulted in neurodegeneration, demonstrating the

necessity of proper dopaminergic handling for neuronal health (Chen et al., 2008). Mice deficient in VMAT2 display indices of cytosolic dopamine metabolism as well as age-dependent nigrostriatal dopaminergic degeneration (Caudle et al., 2007; Taylor et al., 2009; 2014). This work has been replicated in *Drosophila melanogaster* deficient in VMAT expression that display fewer dopaminergic neurons (Lawal et al., 2010), and in adult rats that show dopaminergic degeneration resulting from an acquired loss of VMAT2 in adulthood (Bucher et al., 2020). The purpose of this article is to establish the *cat-1* knockout specifically and the *C. elegans* model in general as a viable model for the role of VMAT as a mediator of synaptic function and neuronal vulnerability.

Single worm PCR and the utility of the hermaphroditic reproduction strategy of these worms allows us to readily identify mutants and perform relevant crosses. Simple breeding schemes allow us to create enough reporter strains to examine the effects of vesicular transporter disruption for the entire *C. elegans* neural network. Western blot and immunofluorescent techniques, though rarely used in *C. elegans* research, provide a valuable way of confirming the presence or absence of a protein and subsequent distribution in relevant tissues that are consistent with methods used in mammalian models.

Despite their many advantages, studies of *C. elegans* focused on the *cat-1*/VMAT protein are limited (Duerr et al., 1999; Young et al., 2018). The importance of *cat-1*/VMAT in the establishment of food detection, feeding rate, and reproduction have been demonstrated in the past and replicated by the genetic and pharmacological interventions used in this study (Duerr et al., 1999; Young et al., 2018). Previous cell ablation studies demonstrate that the slowing down of a worm when on a food source is dependent on the presence of intact dopamine neuronal architecture (Sawin et al., 2000). It is interesting that the loss of functional *cat-1*/VMAT replicates this phenotype with the probable effect of system wide catecholaminergic dysfunction (Figure 3A and Duerr et al., 1999; Young et al., 2018). Indeed, one other group has found the addition of either exogenous serotonin or pramipexole can rescue this behavior in *cat-1*/VMAT mutant strains (Young et al., 2018). Although beyond the scope of this article, further exploration of this behavior may reveal synergistic or antagonistic patterns of catecholamine function. Optimal rates of pharyngeal pumping and egg laying require the input of serotonin (Avery and Horvitz, 1990; Trent et al., 1983). The deficits observed in pharyngeal pumping and egg laying rate seen in the *cat-1(ok411)* mutant and associated pharmacological treatment with the inhibitor reserpine suggest that proper storage and trafficking of endogenous stores of this catecholamine is important for its function.

The synaptic vesicle containing functional VMAT2 provides protection to the cell from both endogenous (oxidized dopamine) and certain exogenous (MPTP) insults (Guillot and Miller, 2009; Spina and Cohen, 1989). The MPTP model of selective toxicity to dopamine neurons is well established and a hallmark of mouse work in the PD field (Meredith and Rademacher, 2011). The *C. elegans* model has been used many times to demonstrate the selective toxicity of MPP⁺ (the active metabolite of MPTP) on dopaminergic architecture, however, to our knowledge no laboratory has tested the effects of MPP⁺ in worms lacking the *cat-1*/VMAT protein (Braungart et al., 2004; Lu et al., 2010; Pu and Le, 2008; Wang et al., 2007; Yao et al., 2011). These findings suggest what we have previously found in mice, namely that levels of VMAT regulate MPTP vulnerability (Lohr et al., 2016). Given the genetic tractability of *C. elegans*, the creation of *cat-1*/VMAT

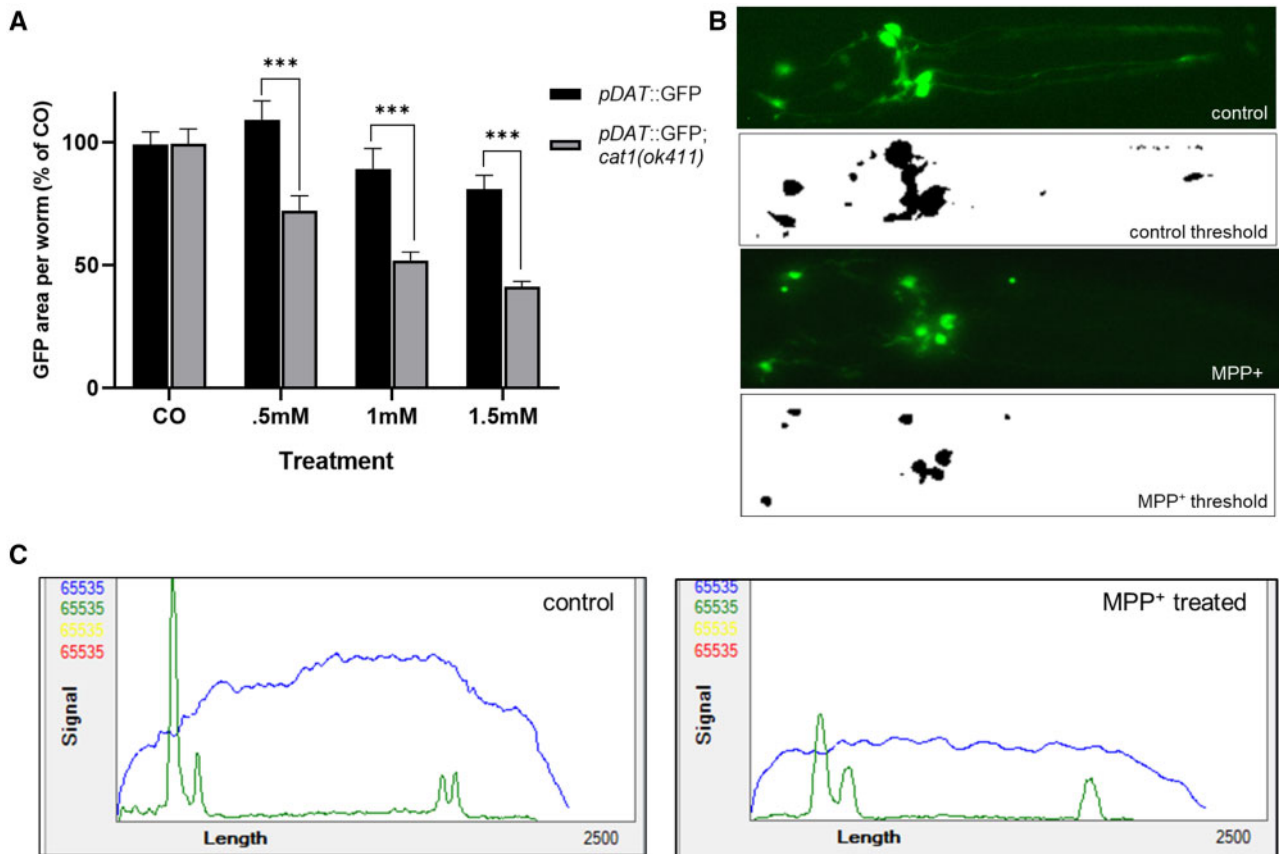


Figure 4. Dopamine neurons lacking the *cat-1*/VMAT transporter are more susceptible to MPP^+ induced neurodegeneration. **A**, Image analysis using automated thresholding shows increased sensitivity of the *cat-1*/VMAT mutant *ok411* to MPP^+ via reduced fluorescent area of dopamine neurons. **B**, Representative fluorescent images of an untreated (control) and MPP^+ treated worm, followed by their transformation to a binary image using the Yen thresholding method (control threshold and MPP^+ threshold) for total area analysis using particle analyzer. **C**, Representative profile graph using the COPAS large particle flow cytometer, green peaks represent intensity values of *dat-1::GFP*, blue signal is extinction, representing the body of the worm. GFP fluorescence driven by the *dat-1* promoter. Sample size for 2-way ANOVA is $n = 587$, comprised of 60–100 worms per group over a series of 4 separate experiments *** $p < .0001$ using Bonferroni's multiple comparisons test following a 2-way ANOVA revealing a significant ($p < .001$) interaction between strain of worm and treatment.

overexpressing worms in future studies is certainly feasible and may facilitate future studies aimed at using enhanced monoamine storage as a therapeutic intervention. It is notable, but not surprising given the evolutionary development of the TEXAN antiporters that the protective effects of monoamine transporters extends across both vertebrate and invertebrate animal models (Figure 1; Schuldiner et al., 1995). This provides further confidence in the utilization of *C. elegans* as a model for vesicular dysfunction related to monoamine transporter efficacy.

C. elegans is gaining support as a model for toxicity testing, demonstrating conserved LD_{50} values and similarities in toxic mechanisms with rodent models (Hunt, 2017). Previous research demonstrates a clear connection between a number of environmental pollutants and the expression of VMAT2 in the nigrostriatal system of mouse models. However, mechanistic studies and full-scale screens of Toxcast libraries are lacking due to the absence of an inexpensive, viable model of monoaminergic vesicular dysfunction. The introduction of the COPAS large particle cytometer may help provide the resolution needed to bring high throughput capability to the screening of potential neurotoxic compounds. Indeed, we are currently refining assays in our lab (Figure 4C). The characterization of the *C. elegans* model of impaired vesicular storage seen in this article is a promising development.

Metabolomics analysis of *cat-1(ok411)* worms showed altered pathways in tyrosine metabolism, possibly resulting from the vesicular mishandling of dopamine in vesicles lacking *cat-1*/VMAT. Members of the pathway suggested lower dopamine levels and higher levels of dopamine metabolites (Supplementary Figure 2). Pathway analysis also suggested changes in glutamate metabolism in worms lacking *cat-1*/VMAT, similar to a previous study that showed altered levels of glutamate detected through NMR metabolomics in the substantia nigra of aged mice expressing low levels of VMAT2 (Salek et al., 2008). MPP^+ enters the neuron through the cell membrane via dopamine transporter 1 (DAT1), thus selectively affecting dopaminergic neurons (Gainetdinov et al. 2002). As such, it was telling to see differences in the metabolism of tyrosine—the precursor of dopamine—in wild-type worms treated with MPP^+ . The finding of differences in tryptophan metabolism is more curious considering that MPP^+ has low affinity for the plasma membrane transporter in serotonin neurons. However, cellular crisis in dopaminergic cells could lead to alterations in tryptophan metabolism reflecting the interdependence of both amines. In fact, these changes in tryptophan metabolism might represent a more generalized response to the increased proteotoxicity involved in cellular degeneration (van der Goot et al. 2012). Likewise, changes in the pentose glucuronate interconversion pathway may also be indicative of a

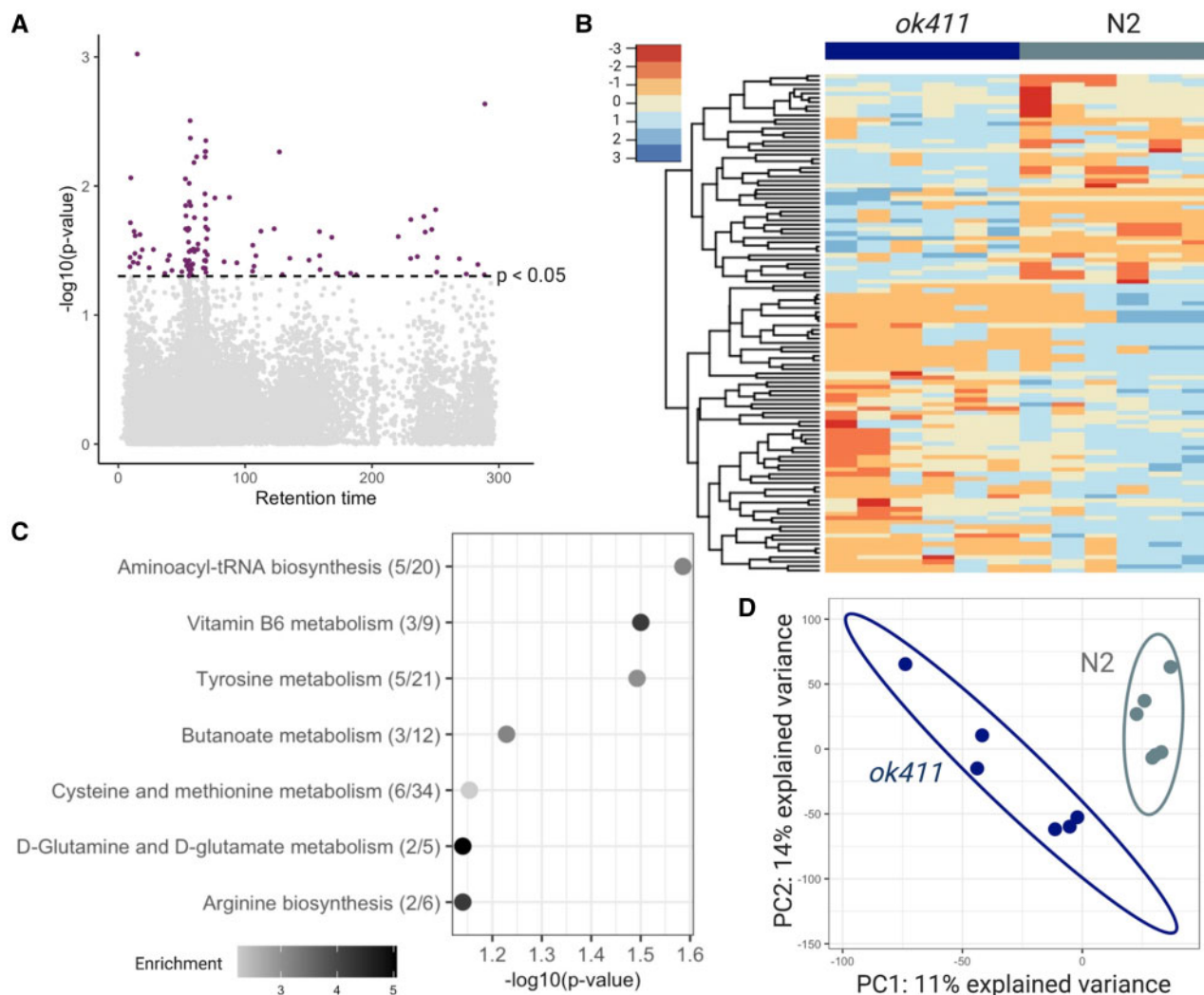


Figure 5. The *cat-1* (*ok411*) strain shows patterns of altered metabolism. **A**, Manhattan plot shows features that were different with $p < .05$ (red) in *cat-1* (*ok411*) mutants compared with wild-type N2 worms. **B**, Hierarchical clustering of features associated with the *cat-1* (*ok411*) mutant with $p < .05$. **C**, Top pathways altered (Fisher's exact test p -value < 0.1) in *cat-1* (*ok411*) worms, analyzed using the Mummichog software. The overlap size of the pathway is indicated in parentheses (number of significant hits/pathway size). The color of the bubbles represent enrichment, calculated as the quotient of total number of hits in the pathway divided by expected number of hits. **D**, Partial least squares discriminant analysis (PLS-DA) comparing *cat-1* (*ok411*) mutants to wild-type N2 worms. $n = 6$ with 500 worms in each sample for both groups.

mitochondrial crisis (Mullarky and Cantley 2015). Features that are altered in both types of dopaminergic neuronal perturbations could provide information on metabolic pathways that are of interest to neuronal damage and degeneration. Although we were able to discover 14 features overlapping between the two conditions, we did not have sufficient power to determine pathways of interest that were altered between the 2 conditions. Future studies could use spectral fragmentation to identify the chemical structure of these 14 features. Further, chemical entities of metabolic relevance can be studied by using an appropriate mutant worm strain or by employing biochemical assays.

High-resolution mass spectrometry-based metabolomics has been used in several *C. elegans* studies (Edison et al., 2015; Hastings et al., 2017; Mor, 2020; Witting et al., 2018). The comprehensive molecular understanding of the nematode model makes it amenable to characterizing systemic biochemistry and perturbations to global metabolism as a result of genetic,

environmental, and toxicological perturbations. Our initial findings suggest that the use of this technique could add to the systems-level evaluation of toxicity in this model. This information may provide further avenues of exploration when looking at metabolic effects of neurodegeneration. In fact, systems-wide approaches to studying common neurodegenerative diseases like PD are recommended by the variety of circuitry affected (Taylor et al., 2011, 2014, 2009). For example, in the few cases of dopamine-serotonin transport disease, a disease related to a mutant allele in VMAT2 known as P387L, patients exhibit developmental delay, parkinsonism, sleep disturbances, mood disorders and a host of issues related to autonomic dysfunction (Rath et al., 2017). The application of high-resolution mass spectrometry allows us to identify metabolic dysfunction in an untargeted manner. The unbiased nature of this approach has the capability of providing links to associated human diseases previously unrecognized. By replicating the dysfunction of monoamine transport and storage in *C. elegans*

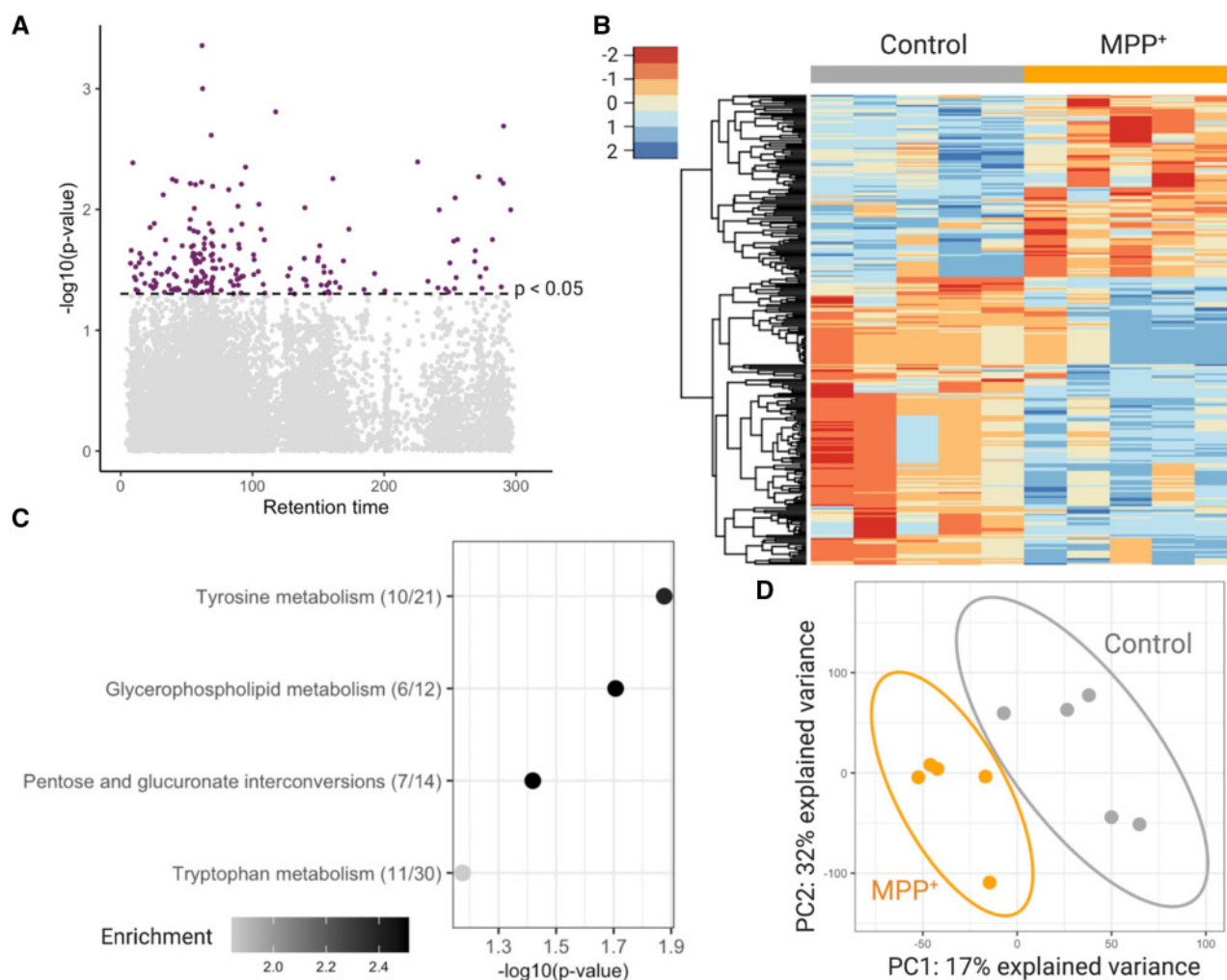


Figure 6. Worms treated with MPP⁺ show patterns of altered metabolism. **A**, Manhattan plot shows features that were different with $p < .05$ (red) N2 worms treated with MPP⁺ compared with untreated N2 worms. **B**, Hierarchical clustering of features associated with treatment with $p < .05$. **C**, Top pathways altered (Fisher's exact test p -value < 0.1) in N2 worms treated with 1 mM MPP⁺, analyzed using the Mummichog software. The overlap size of the pathway is indicated in parentheses (number of significant hits/pathway size). The color of the bubbles represent enrichment, calculated as the quotient of total number of hits in the pathway divided by expected number of hits. **D**, Partial least squares discriminant analysis (PLS-DA) comparing N2 worms with N2 worms treated with 1 mM MPP⁺. $n = 5$ with 500 worms in each sample for both groups.

we may yet uncover similar metabolic signatures of relevant disease in humans. Our group has recently reported that the same high resolution mass spectrometry-based metabolomic platform can identify disease-specific alterations in plasma from patients with and without Alzheimer's disease (Niedzwiecki *et al.*, 2020; Vardarajan *et al.*, 2020) demonstrating the utility of the approach from worms to humans. We expect *C. elegans* will play an important role in future exposome-level studies by providing a laboratory-based validation of observed metabolomic alterations in human disease (Vermeulen *et al.*, 2020). Overlap in common metabolic signatures could potentially be useful for treatment and early diagnosis in neurodegenerative diseases and a number of addiction and mood disorders.

In summary, our results demonstrate the evolutionary-conserved nature of monoamine function in *C. elegans* and further suggest that high-resolution mass spectrometry-based metabolomics can be used in this model to study environmental and genetic contributors to complex human disease.

SUPPLEMENTARY DATA

Supplementary data are available at Toxicological Sciences online.

ACKNOWLEDGMENTS

We would like to acknowledge several members of the *C. elegans* community for their kind assistance. The Katz lab at Emory University, especially Teresa Lee who got us started in the basics of the *C. elegans* model system. Nicholas Stroustrup for providing input on assessment of lifespan. Richard Nass for providing several antibodies, including the *cat-1*/VMAT antibody used in this article. The Edison lab for their hospitality and discussions of worm metabolomics. The Blakely lab for helpful discussions on metabolism in *C. elegans*. Finally, we would like to thank Shuzhao Li for help with Mummichog pathway analysis, and ViLinh Tran and Michael Orr from the Clinical Biomarkers lab at Emory

University for running our metabolomics samples and creating biochemical assays for redox analysis in worms.

FUNDING

National Institute of Environmental Health Sciences (R01ES023839, P30ES019776, P30ES009089, U2CES02656, T32 ES012870, T32 ES007322).

DECLARATION OF CONFLICTING INTERESTS

Dr Miller receives royalties for his book *The Exposome*.

REFERENCES

- Avery, L., and Horvitz, H. R. (1990). Effects of starvation and neuroactive drugs on feeding in *Caenorhabditis elegans*. *J. Exp. Zool.* **253**, 263–270.
- Bolstad, B. M., Irizarry, R. A., Astrand, M., and Speed, T. P. (2003). A comparison of normalization methods for high density oligonucleotide array data based on variance and bias. *Bioinformatics* **19**, 185–193.
- Bradner, J. M., Suragh, T. A., Wilson, W. W., Lazo, C. R., Stout, K. A., Kim, H. M., Wang, M. Z., Walker, D. I., Pennell, K. D., Richardson, J. R., et al. (2013). Exposure to the polybrominated diphenyl ether mixture de-71 damages the nigrostriatal dopamine system: Role of dopamine handling in neurotoxicity. *Exp. Neurol.* **241**, 138–147.
- Braungart, E., Gerlach, M., Riederer, P., Baumeister, R., and Hoener, M. C. (2004). *Caenorhabditis elegans* mpp+ model of Parkinson's disease for high-throughput drug screenings. *Neurodegener. Dis.* **1**, 175–183.
- Brenner, S. (1974). The genetics of *Caenorhabditis elegans*. *Genetics* **77**, 71–94.
- Brighina, L., Riva, C., Bertola, F., Saracchi, E., Fermi, S., Goldwurm, S., and Ferrarese, C. (2013). Analysis of vesicular monoamine transporter 2 polymorphisms in Parkinson's disease. *Neurobiol. Aging* **34**, 1712 e1719–1713.
- Bucher, M. L., Barrett, C. W., Moon, C. J., Mortimer, A. D., Burton, E. A., Timothy Greenamyre, J., and Hastings, T. G. (2020). Acquired dysregulation of dopamine homeostasis reproduces features of Parkinson's disease. *NPJ Parkinson's Dis.* **6**, 34.
- Burton, M. D., Nouri, K., Baichoo, S., Samuels-Toyloy, N., and Kazemi, H. (1994). Ventilatory output and acetylcholine: Perturbations in release and muscarinic receptor activation. *J. Appl. Physiol.* **77**, 2275–2284.
- Caenorhabditis Genetics Center (CGC). (2020). University of Minnesota, Minneapolis, MN. <https://cgc.umn.edu/strain/RB681>. Accessed May 3, 2020.
- Caudle, W. M. (2015). Occupational exposures and Parkinsonism. *Handb. Clin. Neurol.* **131**, 225–239.
- Caudle, W. M., Guillot, T. S., Lazo, C. R., and Miller, G. W. (2012). Industrial toxicants and Parkinson's disease. *Neurotoxicology* **33**, 178–188.
- Caudle, W. M., Richardson, J. R., Wang, M., and Miller, G. W. (2005). Perinatal heptachlor exposure increases expression of presynaptic dopaminergic markers in mouse striatum. *Neurotoxicology* **26**, 721–728.
- Caudle, W. M., Richardson, J. R., Wang, M. Z., Taylor, T. N., Guillot, T. S., McCormack, A. L., Colebrooke, R. E., Di Monte, D. A., Emson, P. C., and Miller, G. W. (2007). Reduced vesicular storage of dopamine causes progressive nigrostriatal neurodegeneration. *J. Neurosci.* **27**, 8138–8148.
- Chen, L., Ding, Y., Cagniard, B., Van Laar, A. D., Mortimer, A., Chi, W., Hastings, T. G., Kang, U. J., and Zhuang, X. (2008). Unregulated cytosolic dopamine causes neurodegeneration associated with oxidative stress in mice. *J. Neurosci.* **28**, 425–433.
- Choi, W. S., Kim, H. W., and Xia, Z. (2015). Jnk inhibition of vmat2 contributes to rotenone-induced oxidative stress and dopamine neuron death. *Toxicology* **328**, 75–81.
- Chong, J., Wishart, D. S., and Xia, J. (2019). Using metaboanalyst 4.0 for comprehensive and integrative metabolomics data analysis. *Curr. Protoc. Bioinformatics* **68**, e86.
- CeDM. (2012). Large-scale screening for targeted knockouts in the *Caenorhabditis elegans* genome. *G3* **2**, 1415–1425.
- Dereeper, A., Guignon, V., Blanc, G., Audic, S., Buffet, S., Chevenet, F., Dufayard, J. F., Guindon, S., Lefort, V., Lescot, M., et al. (2008). Phylogeny.Fr: Robust phylogenetic analysis for the non-specialist. *Nucleic Acids Res.* **36**, W465–469.
- Deupree, J. D., and Weaver, J. A. (1984). Identification and characterization of the catecholamine transporter in bovine chromaffin granules using [3h] reserpine. *J. Biol. Chem.* **259**, 10907–10912.
- Dressler, D., Saberi, F. A., and Barbosa, E. R. (2005). Botulinum toxin: Mechanisms of action. *Arq. Neuropsiquiatr.* **63**, 180–185.
- Duerr, J. S. (2013). Antibody staining in *C. elegans* using “freeze-cracking”. *J. Vis. Exp.* **80**, e50664.
- Duerr, J. S., Frisby, D. L., Gaskin, J., Duke, A., Asermely, K., Huddleston, D., Eiden, L. E., and Rand, J. B. (1999). The *cat-1* gene of *Caenorhabditis elegans* encodes a vesicular monoamine transporter required for specific monoamine-dependent behaviors. *J. Neurosci.* **19**, 72–84.
- Edison, A. S., Clendinen, C. S., Ajredini, R., Beecher, C., Ponce, F. V., and Stupp, G. S. (2015). Metabolomics and natural-products strategies to study chemical ecology in nematodes. *Integr. Comp. Biol.* **55**, 478–485.
- Enayah, S. H., Vanle, B. C., Fuortes, L. J., Doorn, J. A., and Ludewig, G. (2018). Pcb95 and pcb153 change dopamine levels and turn-over in pc12 cells. *Toxicology* **394**, 93–101.
- Fumagalli, F., Gainetdinov, R. R., Wang, Y. M., Valenzano, K. J., Miller, G. W., and Caron, M. G. (1999). Increased methamphetamine neurotoxicity in heterozygous vesicular monoamine transporter 2 knock-out mice. *J. Neurosci.* **19**, 2424–2431.
- Gainetdinov, R. R., Fumagalli, F., Jones, S. R., and Caron, M. G. (2002). Dopamine transporter is required for in vivo MPTP neurotoxicity: Evidence from mice lacking the transporter. *J. Neurochem.* **69**, 1322–1325.
- Glatt, C. E., Wahner, A. D., White, D. J., Ruiz-Linares, A., and Ritz, B. (2006). Gain-of-function haplotypes in the vesicular monoamine transporter promoter are protective for Parkinson disease in women. *Hum. Mol. Genet.* **15**, 299–305.
- Go, Y. M., Walker, D. I., Soltow, Q. A., Uppal, K., Wachtman, L. M., Strobel, F. H., Pennell, K., Promislow, D. E., and Jones, D. P. (2015). Metabolome-wide association study of phenylalanine in plasma of common marmosets. *Amino Acids* **47**, 589–601.
- Goldstein, D. S., Sullivan, P., Holmes, C., Miller, G. W., Alter, S., Strong, R., Mash, D. C., Kopin, I. J., and Sharabi, Y. (2013). Determinants of buildup of the toxic dopamine metabolite dopal in Parkinson's disease. *J. Neurochem.* **126**, 591–603.
- Guillot, T. S., and Miller, G. W. (2009). Protective actions of the vesicular monoamine transporter 2 (vmat2) in monoaminergic neurons. *Mol. Neurobiol.* **39**, 149–170.
- Hastings, J., Mains, A., Artal-Sanz, M., Bergmann, S., Braeckman, B. P., Bundy, J., Cabreiro, F., Dobson, P., Ebert, P., Hattwell, J., et al. (2017). Wormjam: A consensus *C. elegans* metabolic

- reconstruction and metabolomics community and workshop series. *Worm* **6**, e1373939.
- Hastings, T. G., Lewis, D. A., and Zigmond, M. J. (1996). Role of oxidation in the neurotoxic effects of intrastriatal dopamine injections. *Proc. Natl. Acad. Sci. USA* **93**, 1956–1961.
- Hunt, P. R. (2017). The *C. elegans* model in toxicity testing. *J. Appl. Toxicol.* **37**, 50–59.
- Inamdar, A. A., Hossain, M. M., Bernstein, A. I., Miller, G. W., Richardson, J. R., and Bennett, J. W. (2013). Fungal-derived semiochemical 1-octen-3-ol disrupts dopamine packaging and causes neurodegeneration. *Proc. Natl. Acad. Sci. USA* **110**, 19561–19566.
- Lawal, H. O., Chang, H. Y., Terrell, A. N., Brooks, E. S., Pulido, D., Simon, A. F., and Krantz, D. E. (2010). The *Drosophila* vesicular monoamine transporter reduces pesticide-induced loss of dopaminergic neurons. *Neurobiol. Dis.* **40**, 102–112.
- Le Cao, K.-A., Rohart, F., Gonzalez, I., Dejean, S. with key contributors Gautier, B. Bartolo, F. contributions from Monget, P. Coquery, J., Yao, F.Z., and Liquet, B. (2016). Mixomics: Omics data integration project. R package version 6.1.1.
- Li, S., Park, Y., Duraisingham, S., Strobel, F. H., Khan, N., Soltow, Q. A., Jones, D. P., and Pulendran, B. (2013). Predicting network activity from high throughput metabolomics. *PLoS Comput. Biol.* **9**, e1003123.
- Lohr, K. M., Bernstein, A. I., Stout, K. A., Dunn, A. R., Lazo, C. R., Alter, S. P., Wang, M., Li, Y., Fan, X., Hess, E. J., et al. (2014). Increased vesicular monoamine transporter enhances dopamine release and opposes Parkinson disease-related neurodegeneration in vivo. *Proc. Natl. Acad. Sci. USA* **111**, 9977–9982.
- Lohr, K. M., Chen, M., Hoffman, C. A., McDaniel, M. J., Stout, K. A., Dunn, A. R., Wang, M., Bernstein, A. I., and Miller, G. W. (2016). Vesicular monoamine transporter 2 (vmat2) level regulates MPTP vulnerability and clearance of excess dopamine in mouse striatal terminals. *Toxicol. Sci.* **153**, 79–88.
- Lohr, K. M., and Miller, G. W. (2014). Vmat2 and Parkinson's disease: Harnessing the dopamine vesicle. *Expert Rev. Neurother.* **14**, 1115–1117.
- Lohr, K. M., Stout, K. A., Dunn, A. R., Wang, M., Salahpour, A., Guillot, T. S., and Miller, G. W. (2015). Increased vesicular monoamine transporter 2 (vmat2; slc18a2) protects against methamphetamine toxicity. *ACS Chem. Neurosci.* **6**, 790–799.
- Lu, X. L., Yao, X. L., Liu, Z., Zhang, H., Li, W., Li, Z., Wang, G. L., Pang, J., Lin, Y., Xu, Z., et al. (2010). Protective effects of xyloketal b against MPP⁺-induced neurotoxicity in *Caenorhabditis elegans* and pc12 cells. *Brain Res.* **1332**, 110–119.
- Masoud, S. T., Vecchio, L. M., Bergeron, Y., Hossain, M. M., Nguyen, L. T., Bermejo, M. K., Kile, B., Sotnikova, T. D., Siesser, W. B., Gainetdinov, R. R., et al. (2015). Increased expression of the dopamine transporter leads to loss of dopamine neurons, oxidative stress and L-DOPA reversible motor deficits. *Neurobiol. Dis.* **74**, 66–75.
- Meredith, G. E., and Rademacher, D. J. (2011). MPTP mouse models of Parkinson's disease: An update. *J. Parkinsons Dis.* **1**, 19–33.
- Miller, G. W., Kirby, M. L., Levey, A. I., and Bloomquist, J. R. (1999). Heptachlor alters expression and function of dopamine transporters. *Neurotoxicology* **20**, 631–637.
- Miller, K. G., Alfonso, A., Nguyen, M., Crowell, J. A., Johnson, C. D., and Rand, J. B. (1996). A genetic selection for *Caenorhabditis elegans* synaptic transmission mutants. *Proc. Natl. Acad. Sci. USA* **93**, 12593–12598.
- Mor, D. E., Sohrabi, S., Kaletsky, R., Keyes, W., Tartici, A., Kalia, V., Miller, G. W., and Murphy, C. T. (2020). Metformin rescues Parkinson's disease phenotypes caused by hyperactive mitochondria. *Proc. Natl. Acad. Sci. USA* **117**, 26438–26447.
- Mosharov, E. V., Larsen, K. E., Kanter, E., Phillips, K. A., Wilson, K., Schmitz, Y., Krantz, D. E., Kobayashi, K., Edwards, R. H., and Sulzer, D. (2009). Interplay between cytosolic dopamine, calcium, and alpha-synuclein causes selective death of substantia nigra neurons. *Neuron* **62**, 218–229.
- Mullarky, E., and Cantley, L. C. 2015. Diverting glycolysis to combat oxidative stress. In *Innovative Medicine: Basic Research and Development* (K. Nakao, N. Minato, and S. Uemoto, editors), p. 3–23. Tokyo.
- Munoz, P., Huenchuguala, S., Paris, I., and Segura-Aguilar, J. (2012). Dopamine oxidation and autophagy. *Parkinsons Dis.* **2012**, 1–13.
- Niedzwiecki, M. M., Walker, D. I., Howell, J. C., Watts, K. D., Jones, D. P., Miller, G. W., and Hu, W. T. (2020). High-resolution metabolomic profiling of Alzheimer's disease in plasma. *Ann. Clin. Transl. Neurol.* **7**, 36–45.
- Palla, P. 2015. Information management and multivariate analysis techniques for metabolomics data. Doctoral thesis. University of Cagliari, Cagliari, Sardinia, Italy.
- Parsons, S. M. (2000). Transport mechanisms in acetylcholine and monoamine storage. *FASEB J.* **14**, 2423–2434.
- Patel, R., Bradner, J. M., Stout, K. A., and Caudle, W. M. (2016). Alteration to dopaminergic synapses following exposure to perfluorooctane sulfonate (PFOS), in vitro and in vivo. *Med. Sci.* **4**, 13.
- Pham-Lake, C., Aronoff, E. B., Camp, C. R., Vester, A., Peters, S. J., and Caudle, W. M. (2017). Impairment in the mesohippocampal dopamine circuit following exposure to the brominated flame retardant, HBCDD. *Environ. Toxicol. Pharmacol.* **50**, 167–174.
- Porta-de-la-Riva, M., Fontrodona, L., Villanueva, A., and Ceron, J. (2012). Basic *Caenorhabditis elegans* methods: Synchronization and observation. *J. Vis. Exp.* **64**, e4019.
- Prior, C., Marshall, I. G., and Parsons, S. M. (1992). The pharmacology of vesamicol: An inhibitor of the vesicular acetylcholine transporter. *Gen. Pharmacol.* **23**, 1017–1022.
- Pu, P., and Le, W. (2008). Dopamine neuron degeneration induced by MPP⁺ is independent of ced-4 pathway in *Caenorhabditis elegans*. *Cell Res.* **18**, 978–981.
- Rath, M., Korenke, G. C., Najm, J., Hoffmann, G. F., Hagendorff, A., Strom, T. M., and Felbor, U. (2017). Exome sequencing results in identification and treatment of brain dopamine-serotonin vesicular transport disease. *J. Neurol. Sci.* **379**, 296–297.
- Restif, C., Ibanez-Ventoso, C., Vora, M. M., Guo, S., Metaxas, D., and Driscoll, M. (2014). Celest: Computer vision software for quantitative analysis of *C. elegans* swim behavior reveals novel features of locomotion. *PLoS Comput. Biol.* **10**, e1003702.
- Richardson, J. R., Caudle, W. M., Wang, M., Dean, E. D., Pennell, K. D., Miller, G. W., Richardson, J. R., Caudle, W. M., Wang, M., Dean, E. D., et al. (2006). Developmental exposure to the pesticide dieldrin alters the dopamine system and increases neurotoxicity in an animal model of Parkinson's disease. *FASEB J.* **20**, 1695–1697.
- Richardson, J. R., Caudle, W. M., Wang, M. Z., Dean, E. D., Pennell, K. D., and Miller, G. W. (2008). Developmental heptachlor exposure increases susceptibility of dopamine neurons to n-methyl-4-phenyl-1,2,3,6-tetrahydropyridine (MPTP) in a gender-specific manner. *Neurotoxicology* **29**, 855–863.
- Richardson, J. R., and Miller, G. W. (2004). Acute exposure to aroclor 1016 or 1260 differentially affects dopamine transporter and vesicular monoamine transporter 2 levels. *Toxicol. Lett.* **148**, 29–40.

- Salek, R. M., Colebrooke, R. E., Macintosh, R., Lynch, P. J., Sweatman, B. C., Emson, P. C., and Griffin, J. L. (2008). A metabolomic study of brain tissues from aged mice with low expression of the vesicular monoamine transporter 2 (*vmat2*) gene. *Neurochem. Res.* **33**, 292–300.
- Sawin, E. R., Ranganathan, R., and Horvitz, H. R. (2000). *C. elegans* locomotory rate is modulated by the environment through a dopaminergic pathway and by experience through a serotonergic pathway. *Neuron* **26**, 619–631.
- Schindelin, J., Arganda-Carreras, I., Frise, E., Kaynig, V., Longair, M., Pietzsch, T., Preibisch, S., Rueden, C., Saalfeld, S., Schmid, B., et al. (2012). Fiji: An open-source platform for biological-image analysis. *Nat Methods* **9**, 676–682.
- Schuh, R. A., Richardson, J. R., Gupta, R. K., Flaws, J. A., and Fiskum, G. (2009). Effects of the organochlorine pesticide methoxychlor on dopamine metabolites and transporters in the mouse brain. *Neurotoxicology* **30**, 274–280.
- Schuldiner, S., Shirvan, A., and Linial, M. (1995). Vesicular neurotransmitter transporters: From bacteria to humans. *Physiol. Rev.* **75**, 369–392.
- Schymanski, E. L., Jeon, J., Gulde, R., Fenner, K., Ruff, M., Singer, H. P., and Hollender, J. (2014). Identifying small molecules via high resolution mass spectrometry: Communicating confidence. *Environ. Sci. Technol.* **48**, 2097–2098.
- Serrano-Saiz, E., Pereira, L., Gendrel, M., Aghayeva, U., Bhattacharya, A., Howell, K., Garcia, L. R., and Hobert, O. (2017). A neurotransmitter atlas of the *Caenorhabditis elegans* male nervous system reveals sexually dimorphic neurotransmitter usage. *Genetics* **206**, 1251–1269.
- Soltow, Q. A., Strobel, F. H., Mansfield, K. G., Wachtman, L., Park, Y., and Jones, D. P. (2013). High-performance metabolic profiling with dual chromatography-Fourier-transform mass spectrometry (DC-FTMS) for study of the exposome. *Metabolomics* **9**, S132–S143.
- Spina, M. B., and Cohen, G. (1989). Dopamine turnover and glutathione oxidation: Implications for Parkinson disease. *Proc. Natl. Acad. Sci. USA.* **86**, 1398–1400.
- Stokes, A. H., Hastings, T. G., and Vrana, K. E. (1999). Cytotoxic and genotoxic potential of dopamine. *J. Neurosci. Res.* **55**, 659–665.
- Taylor, T. N., Alter, S. P., Wang, M., Goldstein, D. S., and Miller, G. W. (2014). Reduced vesicular storage of catecholamines causes progressive degeneration in the locus ceruleus. *Neuropharmacology* **76**, 97–105.
- Taylor, T. N., Caudle, W. M., and Miller, G. W. (2011). *Vmat2*-deficient mice display nigral and extranigral pathology and motor and nonmotor symptoms of Parkinson's disease. *Parkinsons Dis.* **2011**, 1–9.
- Taylor, T. N., Caudle, W. M., Shepherd, K. R., Noorian, A., Jackson, C. R., Iuvone, P. M., Weinshenker, D., Greene, J. G., and Miller, G. W. (2009). Nonmotor symptoms of Parkinson's disease revealed in an animal model with reduced monoamine storage capacity. *J. Neurosci.* **29**, 8103–8113.
- Trent, C., Tsuing, N., and Horvitz, H. R. (1983). Egg-laying defective mutants of the nematode *Caenorhabditis elegans*. *Genetics* **104**, 619–647.
- Uppal, K., Soltow, Q. A., Strobel, F. H., Pittard, W. S., Gernert, K. M., Yu, T., and Jones, D. P. (2013). Xmsanalyzer: Automated pipeline for improved feature detection and downstream analysis of large-scale, non-targeted metabolomics data. *BMC Bioinformatics* **14**, 15.
- van der Goot, A. T., Zhu, W., Vazquez-Manrique, R. P., Seinstra, R. I., Dettmer, K., Michels, H., Farina, F., Krijnen, J., Melki, R., Buijsman, R. C., et al. (2012). Delaying aging and the aging-associated decline in protein homeostasis by inhibition of tryptophan degradation. *Proc. Natl. Acad. Sci. USA.* **109**, 14912–14917.
- Vardarajan, B., Kalia, V., Manly, J., Brickman, A., Reyes-Dumeyer, D., Lantigua, R., Ionita-Laza, I., Jones, D. P., Miller, G. W., and Mayeux, R. (2020). Differences in plasma metabolites related to Alzheimer's disease, APOE epsilon4 status, and ethnicity. *Alzheimers Dement.* **6**, e12025.
- Vermeer, L. M., Florang, V. R., and Doorn, J. A. (2012). Catechol and aldehyde moieties of 3,4-dihydroxyphenylacetaldehyde contribute to tyrosine hydroxylase inhibition and neurotoxicity. *Brain Res.* **1474**, 100–109.
- Vermeulen, R., Schymanski, E. L., Barabasi, A. L., and Miller, G. W. (2020). The exposome and health: Where chemistry meets biology. *Science* **367**, 392–396.
- Walker, D. I., Perry-Walker, K., Finnell, R. H., Pennell, K. D., Tran, V., May, R. C., McElrath, T. F., Meador, K. J., Pennell, P. B., and Jones, D. P. (2019). Metabolome-wide association study of anti-epileptic drug treatment during pregnancy. *Toxicol. Appl. Pharmacol.* **363**, 122–130.
- Wang, Y. M., Pu, P., and Le, W. D. (2007). Atp depletion is the major cause of MPP+ induced dopamine neuronal death and worm lethality in alpha-synuclein transgenic *C. elegans*. *Neurosci. Bull.* **23**, 329–335.
- Warnes, G. R., Bolker, B., Bonebakker, L., Gentleman, R., Liaw, W. H., Lumley, T., Maechler, M., Magnusson, A., Moeller, S., Schwartz, M., et al. (2009). gplots: various R programming tools for plotting data, R package version 2.1. Available at: <https://CRAN.R-project.org/package=gplots>.
- Wickham, H. 2016. Ggplot2: Elegant graphics for data analysis. Springer-Verlag, New York.
- Wilson, W. W., Onyenwe, W., Bradner, J. M., Nennig, S. E., and Caudle, W. M. (2014). Developmental exposure to the organochlorine insecticide endosulfan alters expression of proteins associated with neurotransmission in the frontal cortex. *Synapse* **68**, 485–497.
- Witting, M., Hastings, J., Rodriguez, N., Joshi, C. J., Hattwell, J. P. N., Ebert, P. R., van Weeghel, M., Gao, A. W., Wakelam, M. J. O., Houtkooper, R. H., et al. (2018). Modeling meets metabolomics—The Wormjam consensus model as basis for metabolic studies in the model organism *Caenorhabditis elegans*. *Front. Mol. Biosci.* **5**, 96.
- Xiong, J., Zhang, X., Huang, J., Chen, C., Chen, Z., Liu, L., Zhang, G., Yang, J., Zhang, Z., Zhang, Z., et al. (2016). Fenpropathrin, a widely used pesticide, causes dopaminergic degeneration. *Mol. Neurobiol.* **53**, 995–1008.
- Yao, X. L., Wu, W. L., Zheng, M. Y., Li, W., Ye, C. H., and Lu, X. L. (2011). Protective effects of lycium barbarum extract against MPP(+)-induced neurotoxicity in *Caenorhabditis elegans* and pc12 cells. *Zhong Yao Cai* **34**, 1241–1246.
- Yen, J. C., Chang, F. J., and Chang, S. (1995). A new criterion for automatic multilevel thresholding. *IEEE Trans. Image Process.* **4**, 370–378.
- Young, A. T., Ly, K. N., Wilson, C., Lehnert, K., Snell, R. G., Reid, S. J., and Jacobsen, J. C. (2018). Modelling brain dopamine-serotonin vesicular transport disease in *Caenorhabditis elegans*. *Dis. Model. Mech.* **11**, dmm035709.
- Yu, T., Park, Y., Johnson, J. M., and Jones, D. P. (2009). Apcms—adaptive processing of high-resolution LC/MS data. *Bioinformatics* **25**, 1930–1936.